MISSOURI S&T

CENTER FOR INFRASTRUCTURE ENGINEERING STUDIES

ASSESSMENT OF KARST ACTIVITY AT SPRINGFIELD ROUTE 60 STUDY SITE

by

Neil L. Anderson

A University Transportation Center Program at Missouri University of Science & Technology

Disclaimer

Technical Report Documentation Page

1. Report No.	2. Government Accession No.	3. Recipient's Catalog No.
UTC R194		

4. Title and Subtitle	5. Report Date
ASSESSMENT OF KARST ACTIVITY AT SPRINGFIELD ROUTE 60 STUDY SITE	February 2008
	6. Performing Organization Code
7. Author/s Neil L. Anderson	8. Performing Organization Report No. 00016982
9. Performing Organization Name and Address Center for Infrastructure Engineering Studies/UTC program Missouri University of Science & Technology 223 Engineering Research Lab Rolla, MO 65409	10. Work Unit No. (TRAIS) 11. Contract or Grant No. DTRS98-G-0021
12. Sponsoring Organization Name and Address U.S. Department of Transportation Research and Special Programs Administration 400 7th Street, SW Washington, DC 20590-0001	13. Type of Report and Period Covered Final 14. Sponsoring Agency Code

15. Supplementary Notes

16. Abstract

MST proposes to acquire electrical resistivity data within a roadway ROW. These geophysical data will be processed, analyzed and interpreted with the objective of locating and mapping any subsurface voids that might compromise the integrity of the pipeline/roadway. The main project deliverable will be a map showing the location and estimated depth of any voids.

17. Key Words	18. Distribution Statement
Non-destructive imaging, non-invasive imaging, technology transfer, education	No restrictions. This document is available to the public through the National Technical Information Service, Springfield, Virginia 22161.

19. Security Classification (of this report)	20. Security Classification (of this page)	21. No. Of Pages	22. Price
unclassified	unclassified	17	

Form DOT F 1700.7 (8-72)

ASSESSMENT OF KARST ACTIVITY AT SPRINGFIELD ROUTE 60 STUDY SITE

Neil L. Anderson (nanders@umr.edu)

Department of Geological Engineering and Sciences
127 McNutt Hall, Missouri University of Science & Technology, Rolla, MO 65409

EXECUTIVE SUMMARY

Six electrical resistivity profiles were acquired along separate parallel traverses at the Route 60 study site in Springfield, Missouri. Analysis of the acquired geophysical data supports the conclusion that limestone bedrock the study area is dissected by numerous near-orthogonal solution-widened joint sets that trend NNW and ENE, respectively. All of the more visually-prominent solution-widened joints imaged on the resistivity profiles are interpreted as clay-filled; several extend to depths of more than 50 ft (below regional top-of-bedrock). None of the solution-widened joints appears to be air-filled.

INTRODUCTION

Six electrical resistivity profiles (A through F, inclusive) were acquired along parallel traverses at the Springfield Missouri Route 60 study site in an effort to image and characterize the shallow subsurface (to depths of 60 ft) along a proposed segment of new Route 60 (Figure 1).

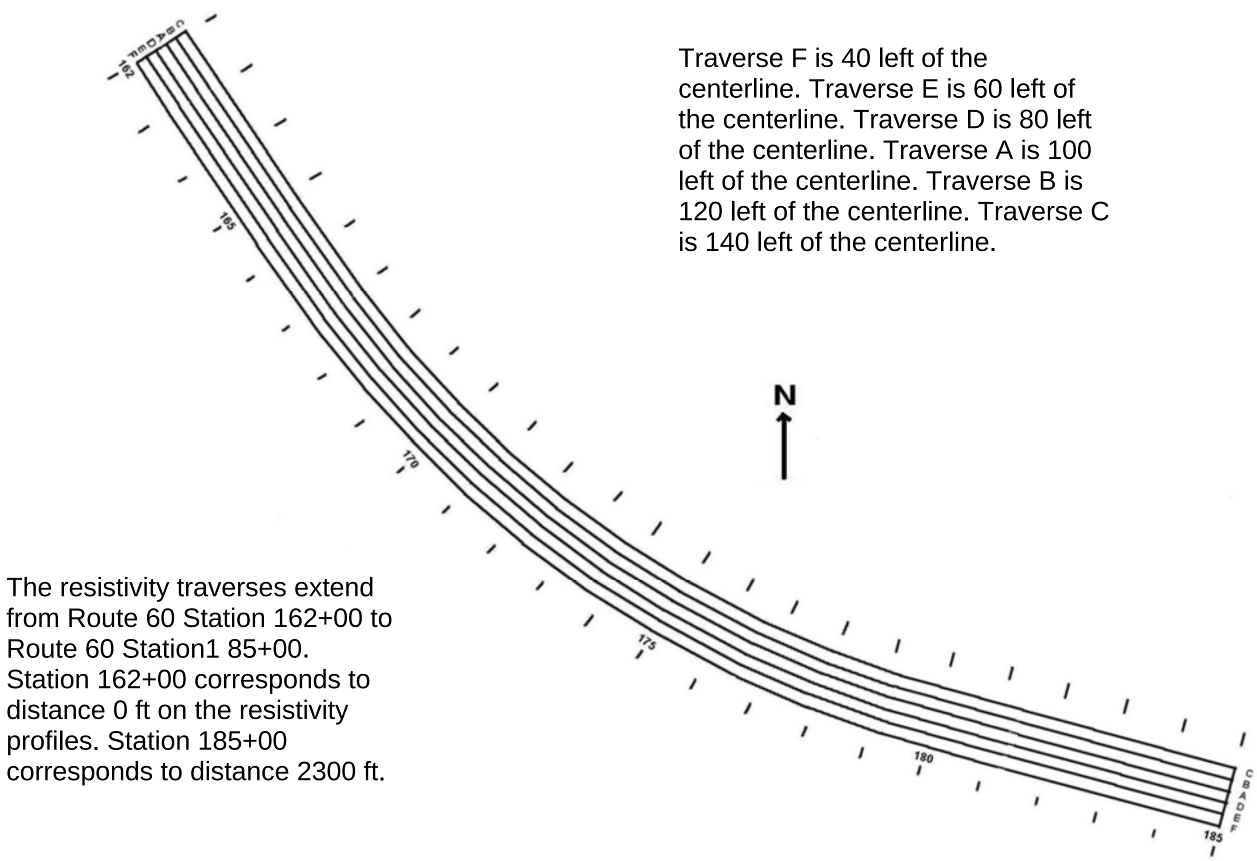

Figure 1: Location of six electrical resistivity traverses relative to centerline of US Route 60.

The primary objective of the geophysical investigation was to determine if air-filled cavities of probable karstic origin are present beneath any of the six traverses (Figure 1). Secondary objectives were: 1) to identify, locate and map prominent solution-widened joints, and 2) to estimate depth to and variable elevation of bedrock along the lengths of the resistivity traverses. The electrical resistivity tool was employed because it is uniquely designed to image air-filled voids, and to differentiate soil, rock and infill clay.

ELECTRICAL RESISTIVITY DATA

Two-dimensional electrical resistivity profiling is commonly used to image the shallow subsurface (depths <100 ft) in karst terrain because air-filled voids, non-clay soil, moist clay, intensely weathered rock, fractured rock and intact rock can normally be differentiated and mapped on 2-D resistivity profiles (Figure 2) (Anderson et al., 2006; FHWA, 2003). Moist clays in SW Missouri are normally characterized by low resistivities (variable, depending on moisture content, purity, and unit shape/size, but usually less than 50 ohm-m). Moist soil and extremely weathered rock (intermixed with clay) is typically characterized by resistivities of between 50 and 150 ohm-m. Dry soil is characterized by resistivities greater than 150; fractured to intact limestone (with minimal clay) is typically characterized by even higher resistivites (typically more than 150 ohm-m, but variable depending on layer thickness, moisture content and impurities). Air-filled voids are normally characterized by very high resistivities (typically >10000 ohm-m, but variable depending on the conductivity of the encompassing strata and depth/size/shape of void).

The resistivity tool frequently provides a superior combination of spatial resolution and depth of investigation in karst terrain than any other non-invasive geophysical imaging technique. The resolution provided by the resistivity tool is a function of the electrode spacing, and other factors including subsurface heterogeneity and conductivity contrasts. During processing, the subsurface beneath the traverse is subdivided into rectangular pixels with lateral dimensions equal to the electrode spacing and vertical dimensions that are typically 25% (at shallowest depths) to 100% (at greatest depths) of the electrode spacing. Pixel size is one estimate of maximum spatial resolution. Additionally, the processing software assumes the subsurface is uniform in directions perpendicular to the traverse; hence some lateral and vertical smoothing (mixing) will occur in heterogeneous strata. The depth of investigation is a function of the length of the 2-D array employed. Maximum depths of investigation are typically 20 to 25% of the array length, varying primarily as a function of subsurface conductivities.

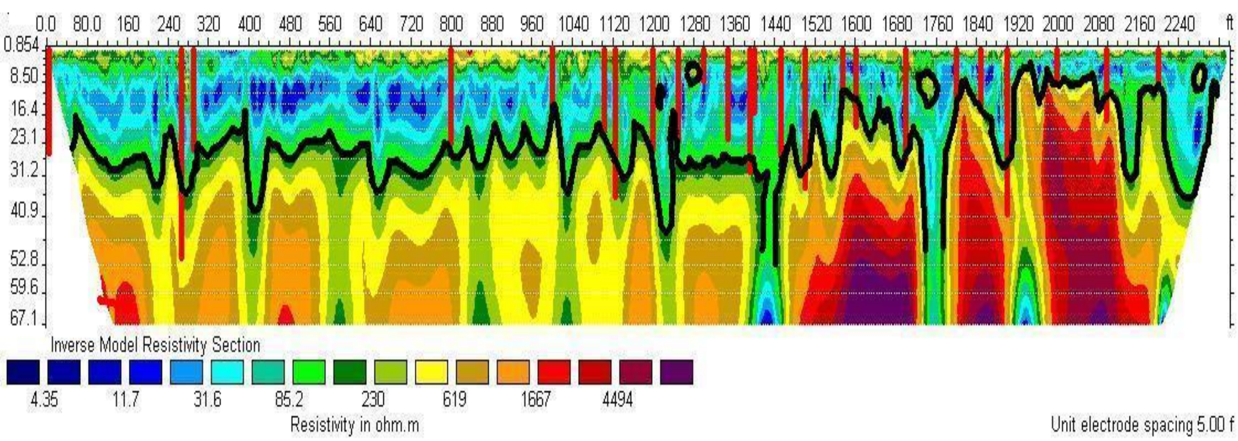

Figure 2: Example resistivity profile. Moist clays in SW Missouri are typically characterized by low resistivities (variable, depending on moisture content, purity, and unit shape/size, but usually less than 50 ohm-m). Moist soil and intensely weathered rock (intermixed with clay) is typically characterized by resistivities of between 50 and 150 ohm-m. Dry soil is characterized by resistivities greater than 150; fractured to intact limestone (with minimal clay) is typically characterized by even higher resistivites (typically more than 150 ohm-m, but variable depending on layer thickness, moisture content and impurities). Air-filled voids are normally characterized by very high resistivities (typically >10000 ohm-m, but variable depending on the conductivity of the encompassing strata and depth/size/shape of void).

ELECTRICAL RESISTIVITY PROFILES: INTERPRETATION

Uninterpreted and interpreted versions of the six electrical resistivity profiles are presented as Figures 3 to 8, respectively. The top of bedrock on the interpreted profiles corresponds approximately to the 150 ohm-m contour value. The reasonableness of these interpretations is confirmed by the correlations presented in Table 1. As noted in Table 1, borehole depths to bedrock and resistivity estimated depths to bedrock are comparable, except where the boreholes are presumed to have terminated in shallow limestone lenses and/or boulders that do not actually constitute top-of-rock (i.e., 179+00; 100' left location; 175+00; 100' left location; Table 1).

The most significant conclusion that can be drawn on the basis of the analyses of resistvity profiles A-F (Figures 3 to 8) is that none of the traverses overlie air-filled voids that are large enough or shallow enough to be imaged on these data. A secondary conclusion is that the resistivity profiles cross two prominent sets of near-orthogonal (NNW-trending and ENE-trending) solution-widened joints (Figures 9 and 10). The orientation of the two sets of solution-widened joints is most clearly identifiable on the structure-contour map of Figure 10. Several of the more prominent solution-widened joints are clay-filled and extend to depths of more than 50 ft (below regional top-of-bedrock). (Note that the widths of the solution-widened joints are visually exaggerated on the electrical resistivity profiles because the traverses do not cross the joint sets at right angles; Figures 3-9.)

Another secondary conclusion is that bedrock is typically anomalously structurally low where solution-widened joints are present (Figures 10 and 11), presumably because of the preferential erosion of weaker rock and/or karstic subsidence.

SUMMARY

The analyses of the acquired geophysical data support the conclusion that study area is dissected by numerous near-orthogonal solution-widened joint sets that trend NNW and ENE, respectively. Several of the more prominent solution-widened joints are clay-filled and extend to depths of more than 50 ft (below regional top-of-bedrock). None of the solution-widened joints appears to be air-filled.

REFERENCES

Anderson, N., Apel, D., Dezelic, V., Ismail, A. and Kovin, O., 2006, Assessment of Karst Activity at Highway Construction Sites in Greene and Jefferson Counties, Missouri, using the Electrical Resistivity Method, proceedings of the Highway Geophysics – NDE conference, St. Louis, MO.

FHWA, 2004, Application of Geophysical Methods to Highway Related Problems, FHWA-sponsored website: www.cflhd.gov/agm/index.htm.

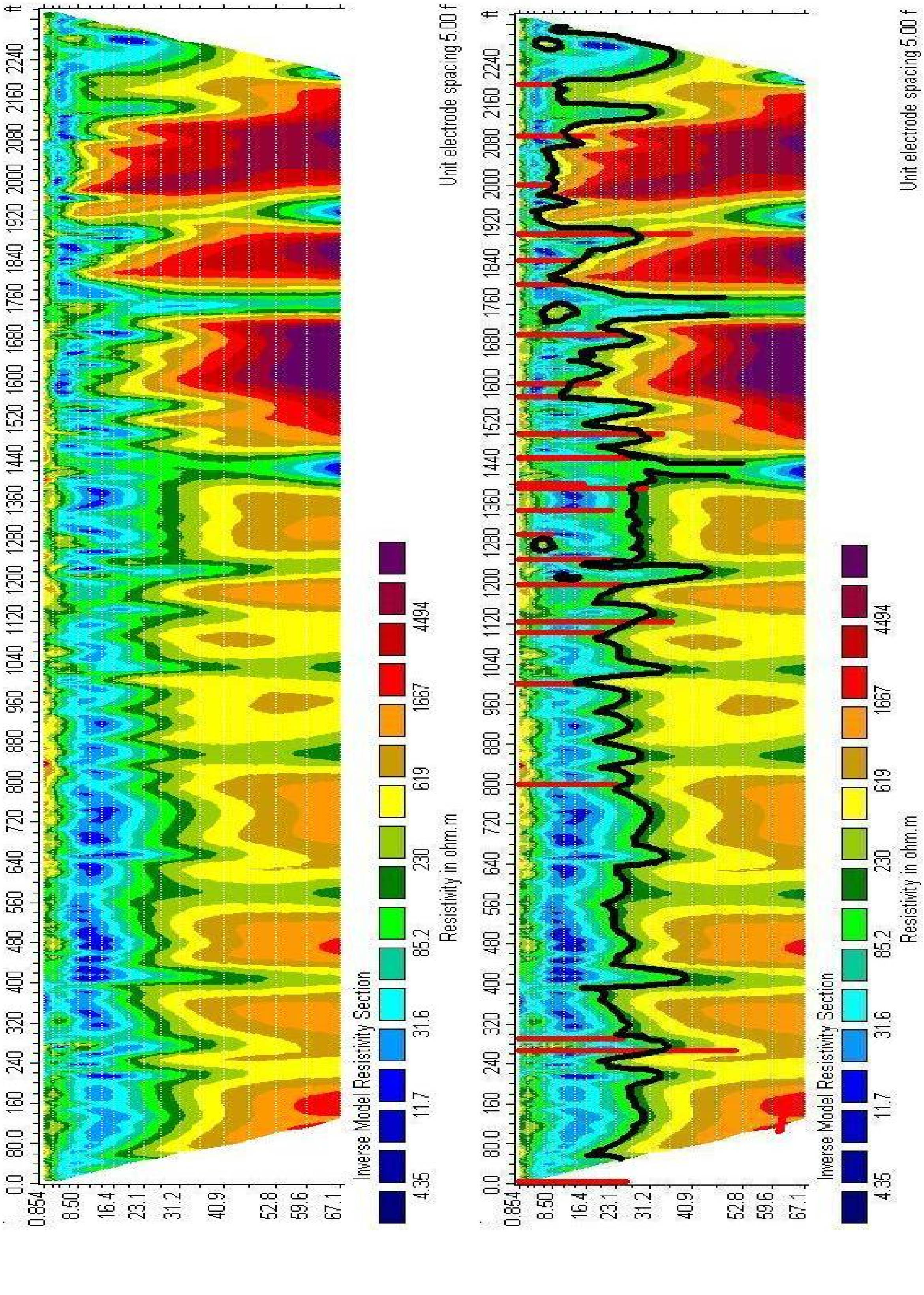

Figure 3: Uninterpreted and interpreted versions of resistivity Profile A (Figure 1). The top of bedrock (black line) correlates reasonably well with the 150 ohm-m contour interval. Borehole locations have been superposed in red. Distance 0 ft on the resistivity profile corresponds with Route 60 Station 62+00; Distance 2300 ft corresponds with Station 85+00 (Figure 1).

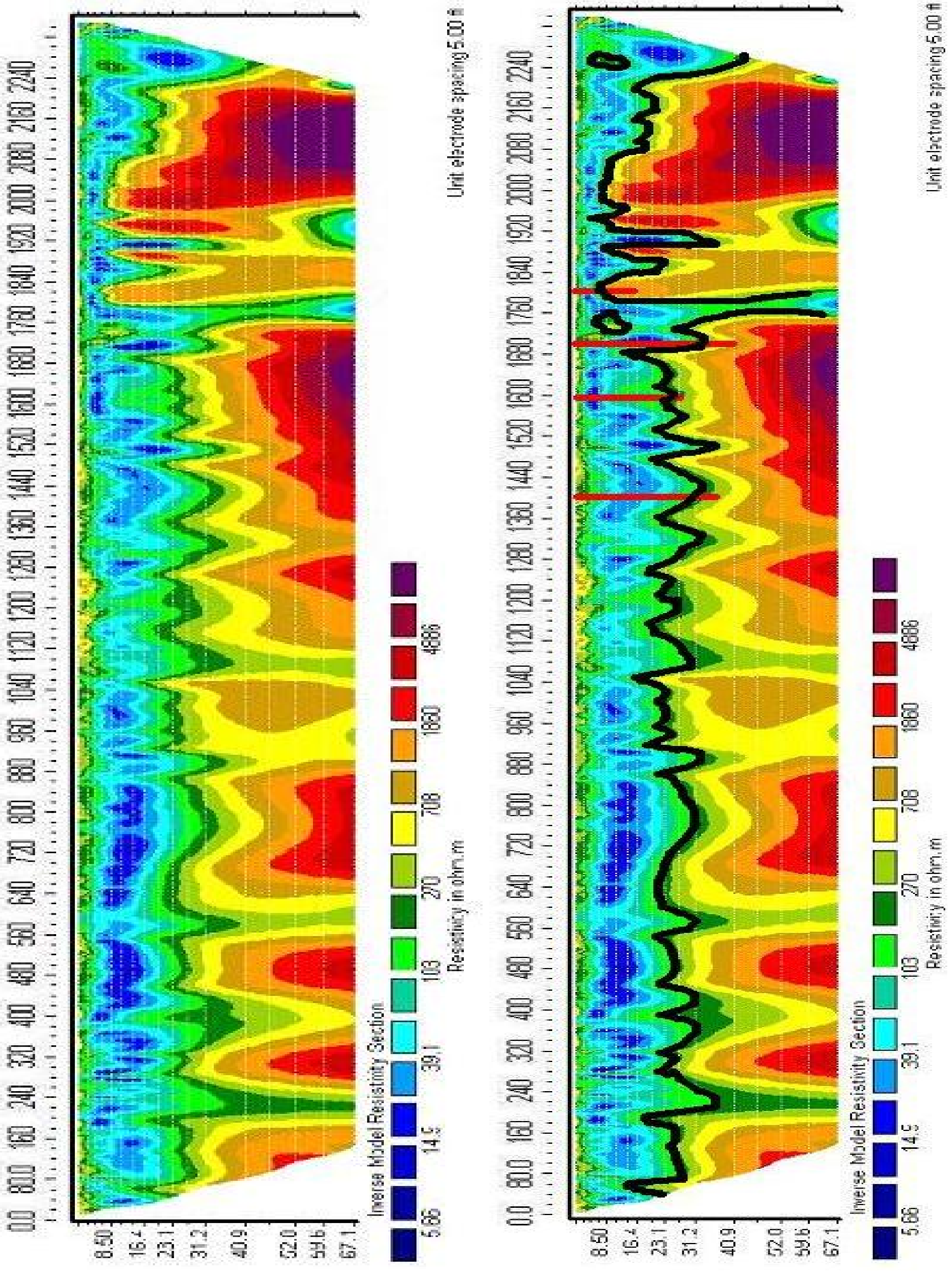

Figure 4: Uninterpreted and interpreted versions of resistivity Profile B (Figure 1). The top of bedrock (black line) correlates reasonably well with the 150 ohm-m contour interval. Borehole locations have been superposed in red. Distance 0 ft on the resistivity profile corresponds with Route 60 Station 62+00; Distance 2300 ft corresponds with Station 85+00 (Figure 1).

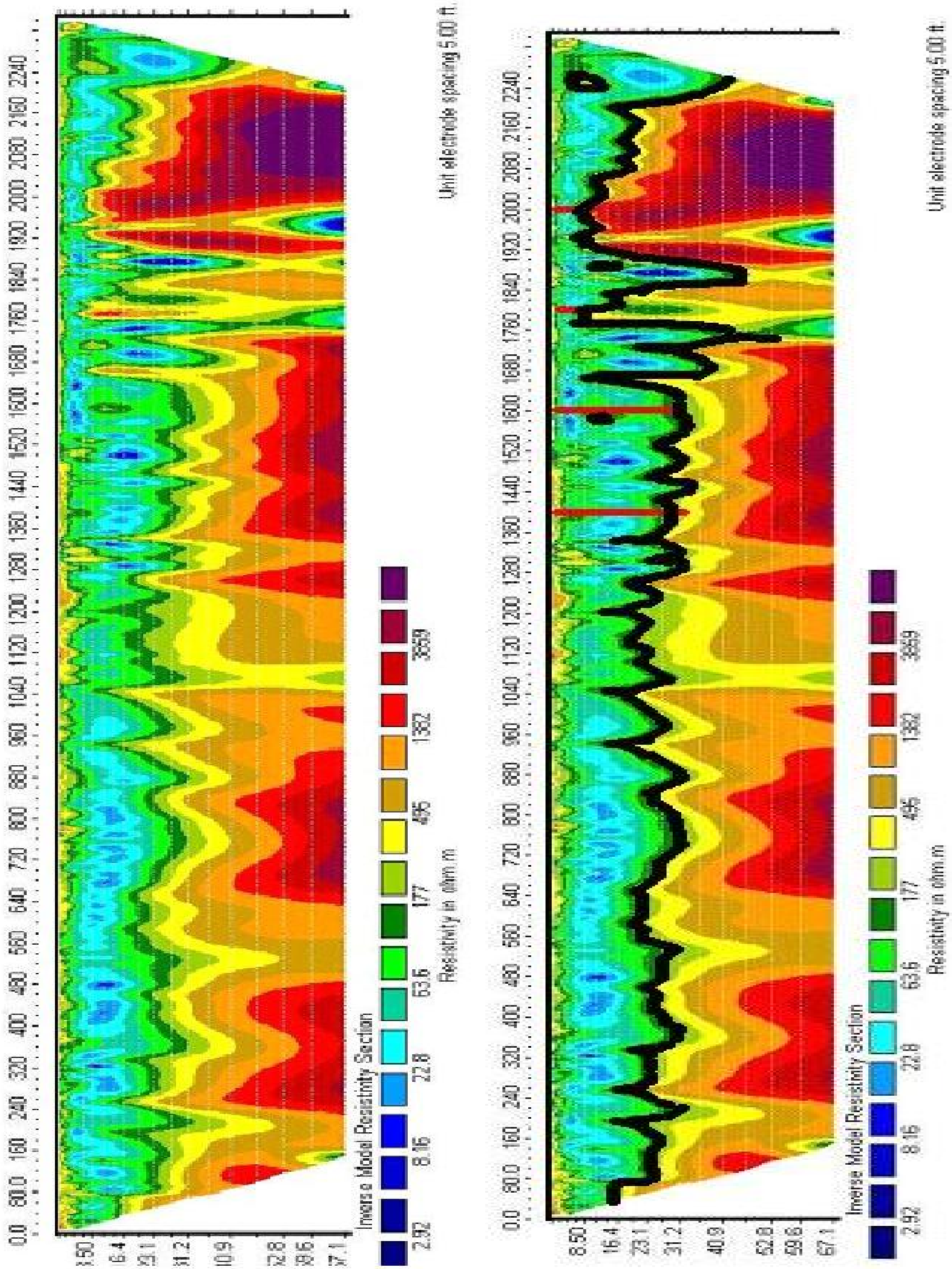

Figure 5: Uninterpreted and interpreted versions of resistivity Profile C (Figure 1). The top of bedrock (black line) correlates reasonably well with the 150 ohm-m contour interval. Borehole locations have been superposed in red. Distance 0 ft on the resistivity profile corresponds with Route 60 Station 62+00; Distance 2300 ft corresponds with Station 85+00 (Figure 1).

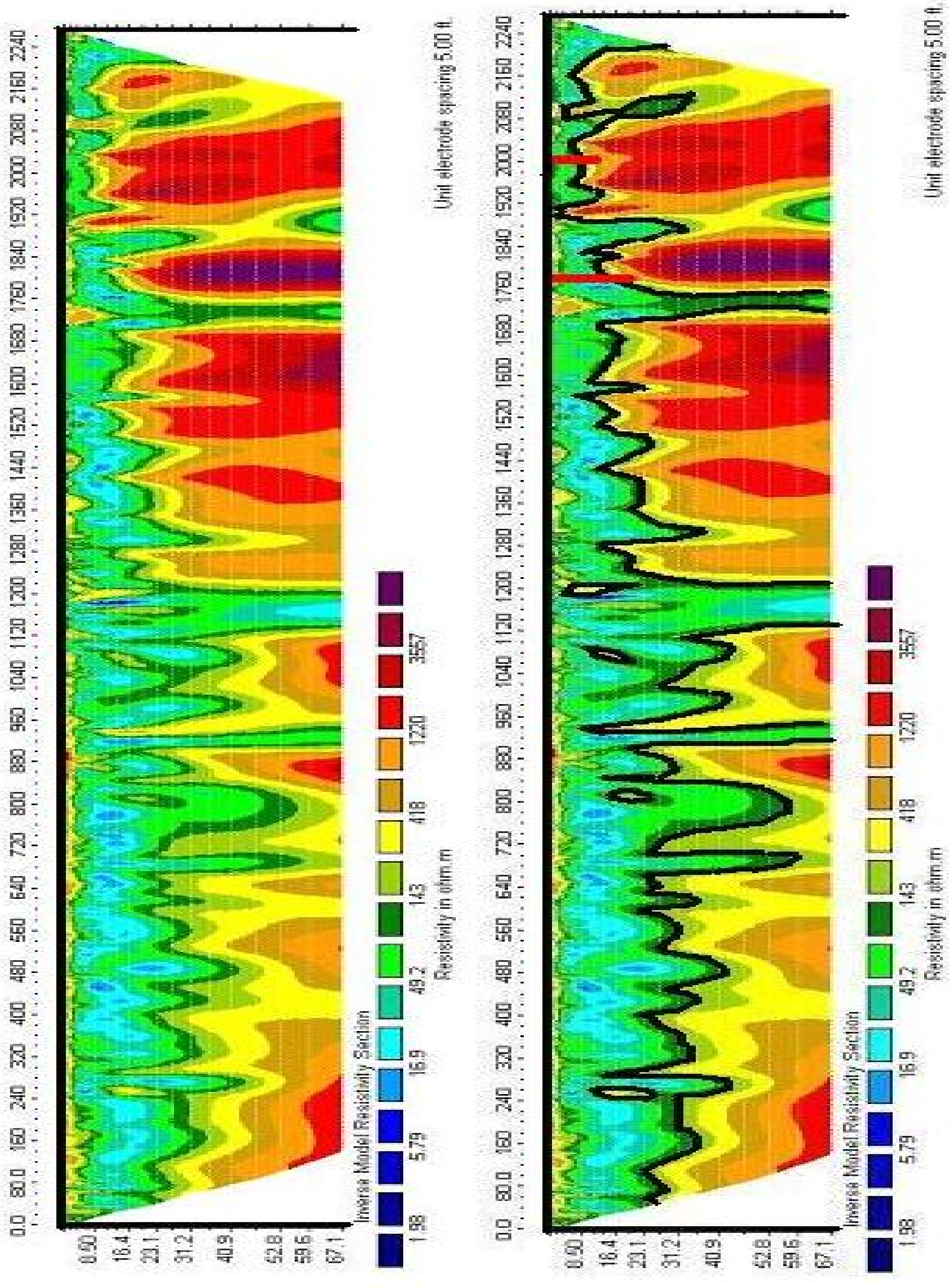

Figure 6: Uninterpreted and interpreted versions of resistivity Profile D (Figure 1). The top of bedrock (black line) correlates reasonably well with the 150 ohm-m contour interval. Borehole locations have been superposed in red. Distance 0 ft on the resistivity profile corresponds with Route 60 Station 62+00; Distance 2200 ft corresponds with Station 84+00 (Figure 1).

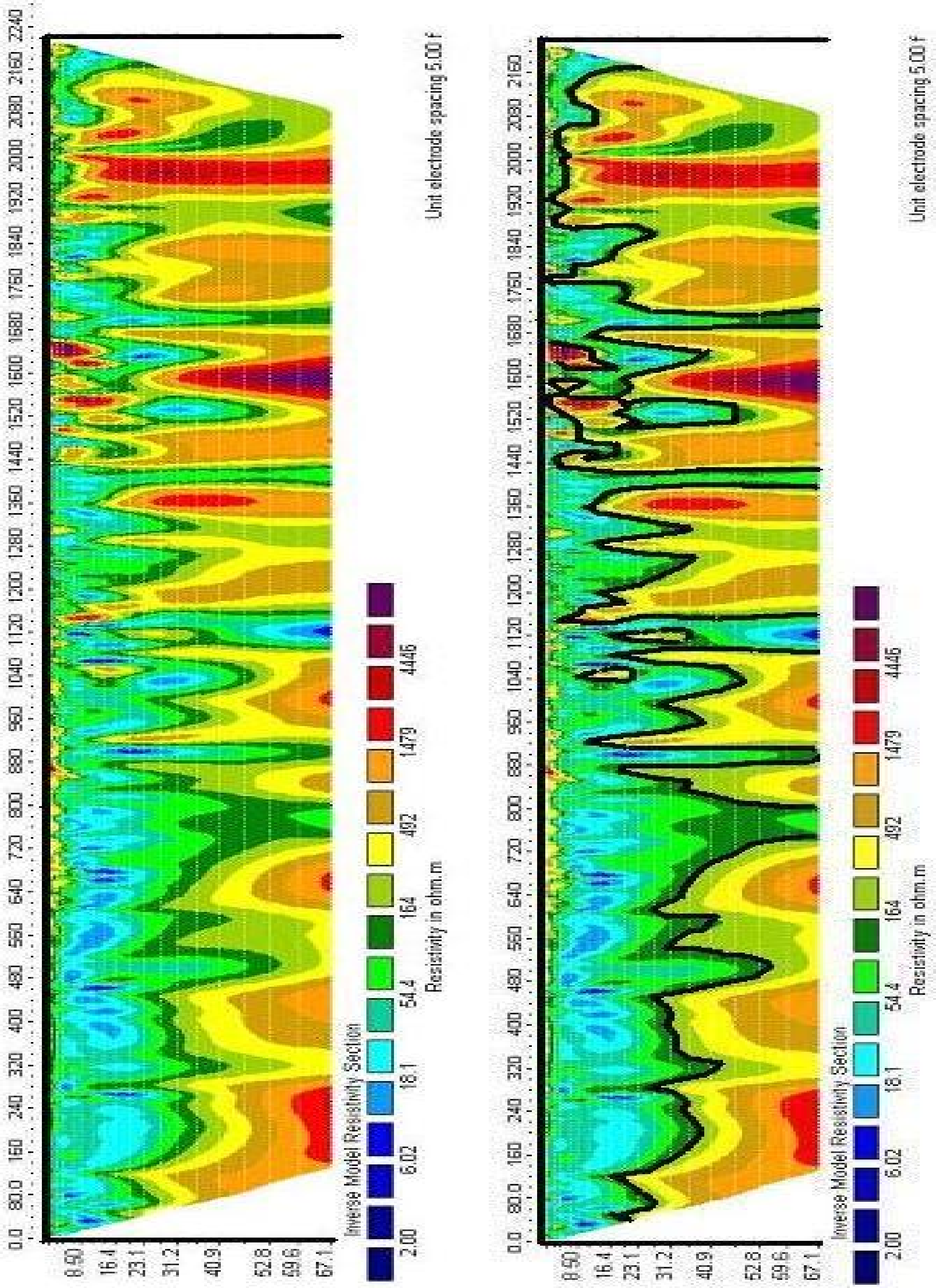

Figure 7: Uninterpreted and interpreted versions of resistivity Profile E (Figure 1). The top of bedrock (black line) correlates reasonably well with the 150 ohm-m contour interval. Distance 0 ft on the resistivity profile corresponds with Route 60 Station 62+00; Distance 2200 ft corresponds with Station 84+00 (Figure 1).

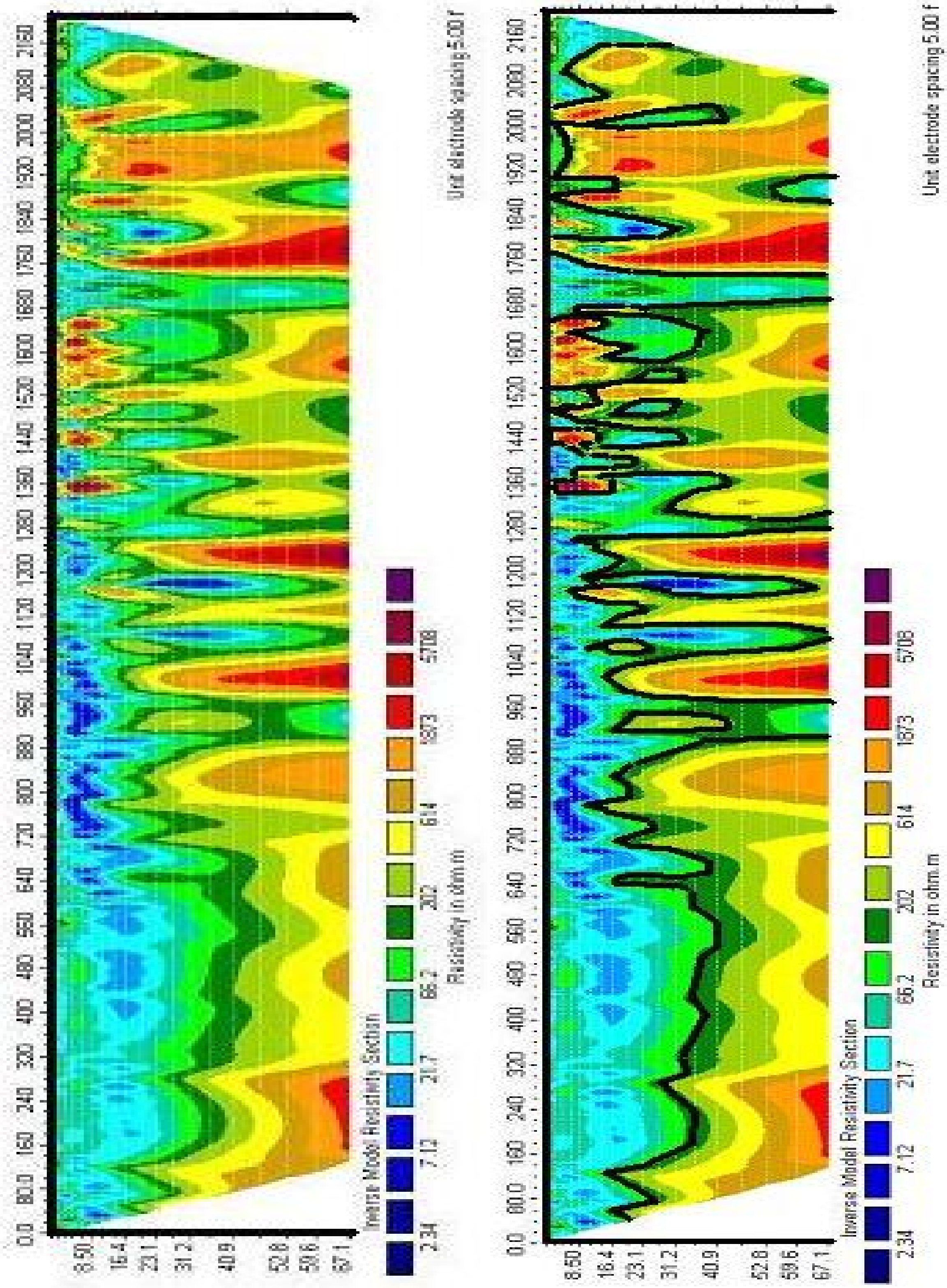

Figure 8: Uninterpreted and interpreted versions of resistivity Profile F (Figure 1). The top of bedrock (black line) correlates reasonably well with the 150 ohm-m contour interval. Distance 0 ft on the resistivity profile corresponds with Route 60 Station 62+00; Distance 2200 ft corresponds with Station 84+00 (Figure 1).

(offset)	(feet)	(feet)	(feet)	
162+00; 100' left	26.4	A; 0	?	Not imaged on resistivity profile

164+65; 100’ left	31.6	A; 265	31	
164+90; 95” left	13.8	A; 290	24	Borehole slightly off line
170+00; 100’ left	22.9	A; 800	23	
172+00; 100’ left	11.7	A; 1000	13	
173+05; 100” left	21.2	A; 1105	20	
173+20; 100’ left	31.8	A; 1120	27	Flank of fracture
174+00; 100’ left	23.0	A; 1200	24	
174+50; 100’ left	22.6	A; 1250	20	
175+00; 100’ left	8.5	A; 1300	6	Appears to have intersected a limestone lense or boulder – not bedrock
175+50; 100’ left	?	A; 1350	27	Borehole TD at 20.2’
176+00; 100’ left	15.4	A; 400	25	BR at 22 ft 10’ from line (see next entry)
176+00; 110’ left	22.0	A; 400	25	
176+00; 120’ left	24.1	B; 1400	27	
176+00; 150 left	27.9	C; 1400	28	
176+50; 100’left	22.4	A; 1450	25	Flank of fracture
177+00; 100’ left	35.6	A; 1500	30	Flank of fracture?
177+75; 100’ left	12.1	A; 1575	10	
178+00; 85’ left	17.3	D; 1600	17	
178+00; 100’ left	11.3	A; 1600	11	
178+00; 120’ left	17.2	B; 1600	20	
178+00; 150’ left	>36.0	C; 1600	30	BH did not encounter bedrock BH is off-line
179+00; 100’ left	7.5 (boulder)	A; 1700	27	Borehole encountered boulder (See next entry)
179+00; 110’ left	29.9	A; 1700	27	Between profiles A and B Ties both well
179+00; 110’ left	29.9	B; 1700	30	
180+00; 100’ left	13.4	A; 1800	12	
180+00; 110’ left	12.5	A; 1800	12	Between profiles A and B Ties A better
180+00; 110’ left	12.5	B; 1800	6	
180+00; 150’ left	4.5	C; 1800	5	
180+50; 100’ left	11.9	A; 1850	13	
181+00; 100’ left	41.4	A; 1900	27	Flank of fracture
182+00; 80’ left	6.4	D; 2000	6	
182+00; 100’ left	8.7	A; 2000	8	
182+00; 150’ left	6.5	C; 2000	6	
182+10; 150’ left	9.3	C; 2010	7	
183+00; 100’ left	18.3	A; 2100	11	
184+00; 100’ left	6.5	A; 2200	8	

Table 1: Estimated depths to bedrock. A comparison of borehole results and resistivity interpretations.

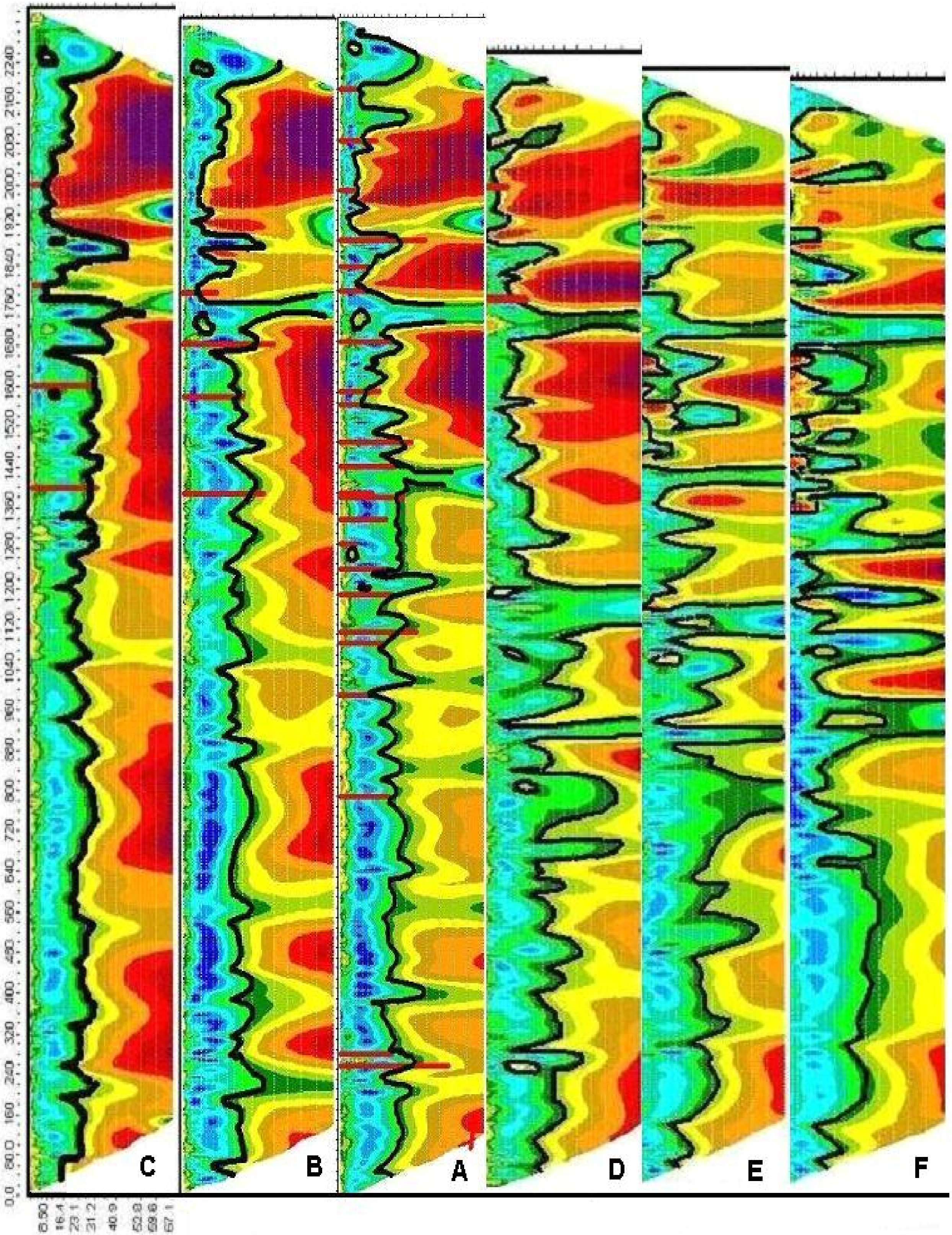

Figure 9: Interpreted resistivity profiles C, B, A, D, E and F arranged in proper left-to-right sequence relative to Route 60 centerline (Figure 1).

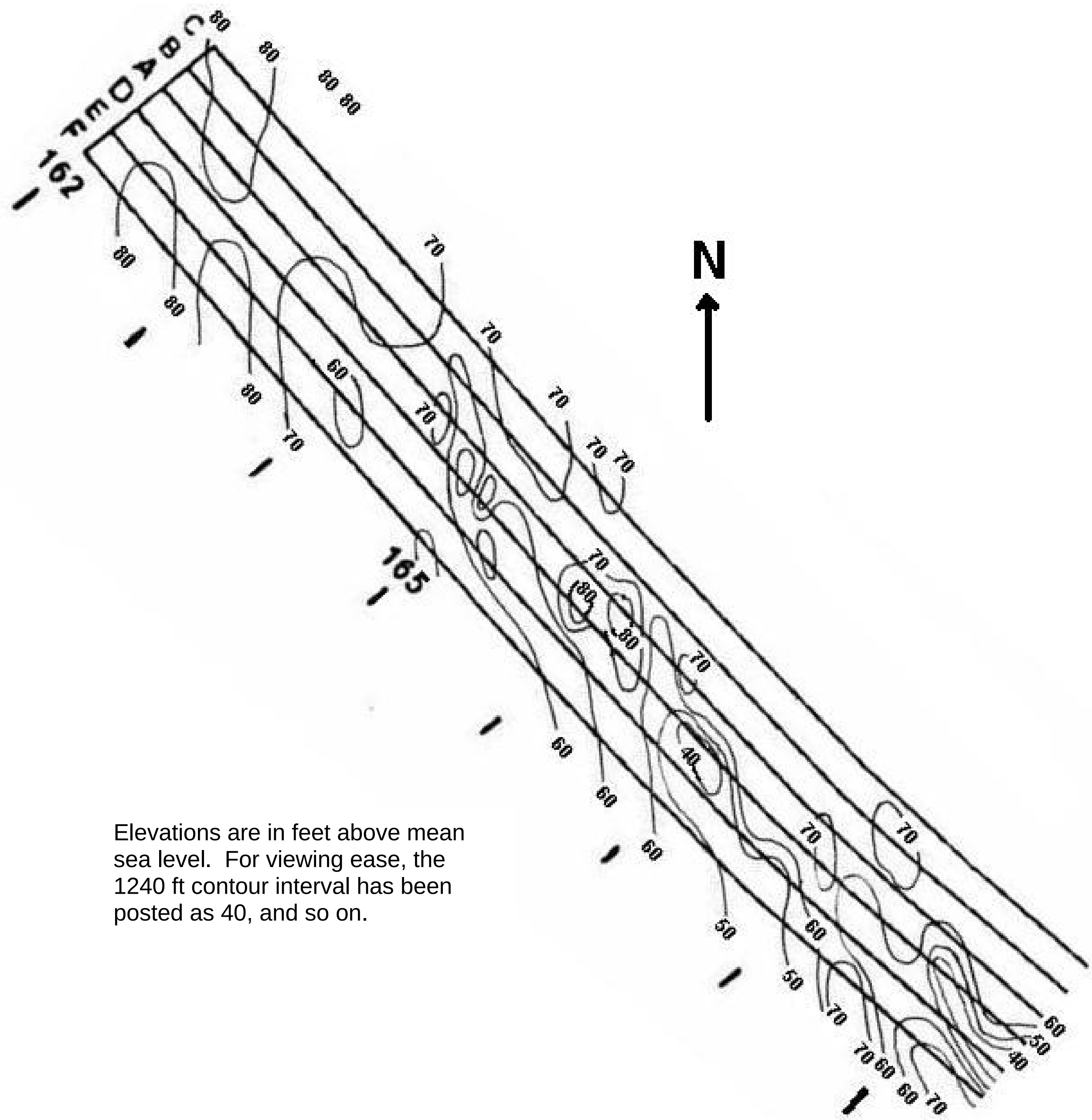

Figure 10a: Contoured top of bedrock elevation map. Segment 1 of 4 (Station 162+00 to Station 169+00; Figure 1). Elevations were posted at 25 ft intervals, hence some of the small-scale features observed on the respective resistivity profiles may not be present on the contoured map. To enhance the quality of the display, the extremely tight contour values associated with fractures that extend below the base of zone imaged on the resistivity profiles are not shown.

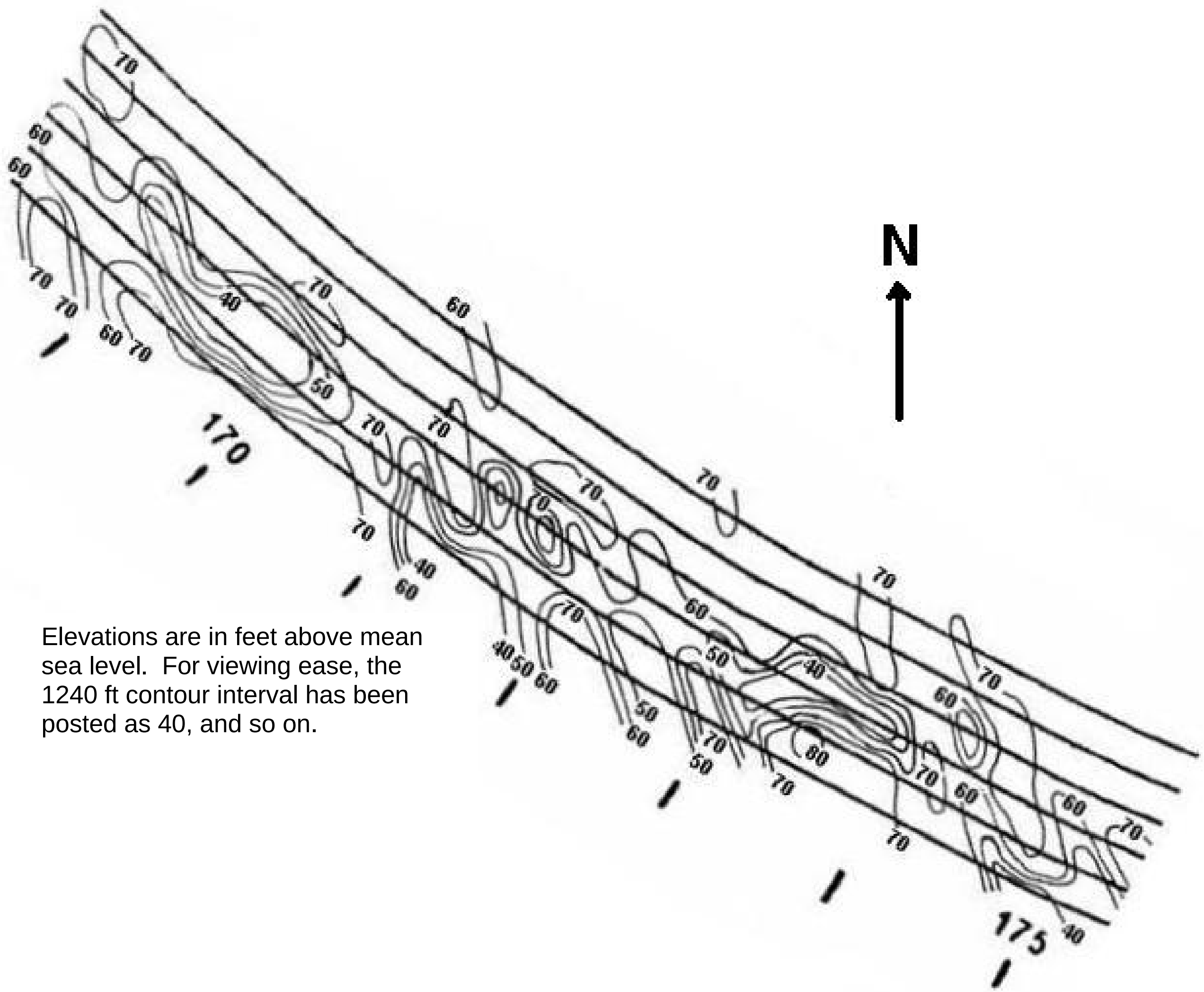

Figure 10b: Contoured top of bedrock elevation map. Segment 2 of 4 (Station 169+00 to Station 175+00; Figure 1). Elevations were posted at 25 ft intervals, hence some of the small-scale features observed on the respective resistivity profiles may not be present on the contoured map. To enhance the quality of the display, the extremely tight contour values associated with fractures that extend below the base of zone imaged on the respective resistivity profiles are not shown.

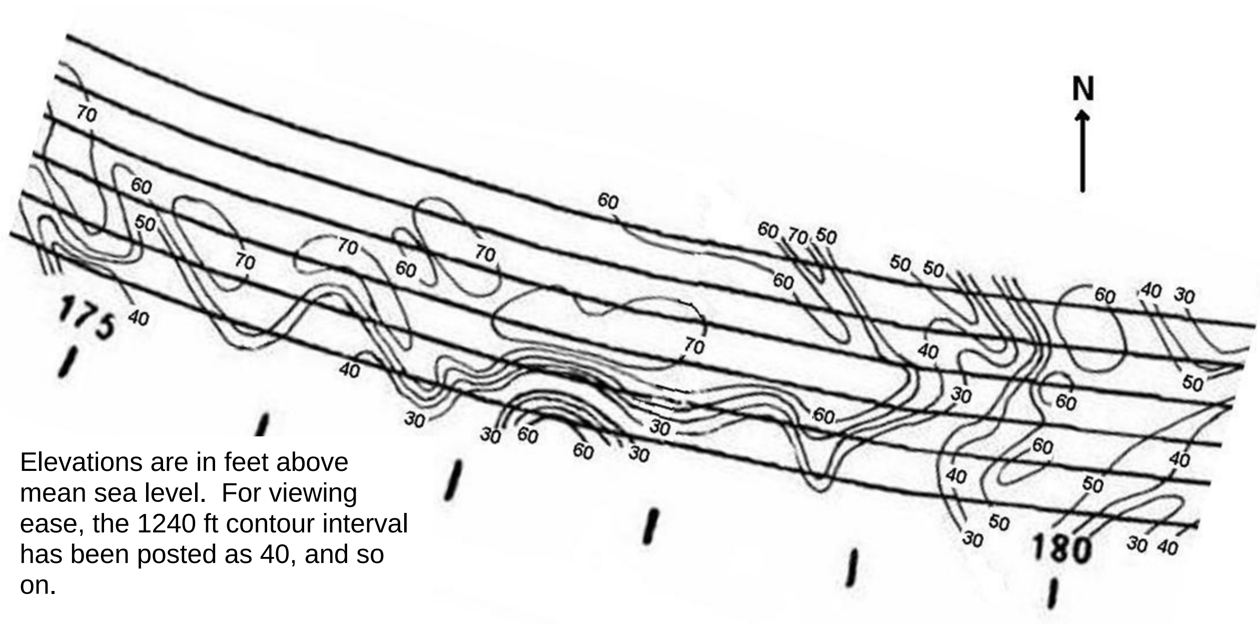

Figure 10c: Contoured top of bedrock elevation map. Segment 3 of 4 (Station 175+00 to Station 182+00; Figure 1). Elevations were posted at 25 ft intervals, hence some of the small-scale features observed on the respective resistivity profiles may not be present on the contoured map. To enhance the quality of the display, the extremely tight contour values associated with fractures that extend below the base of zone imaged on the resistivity profiles are not shown.

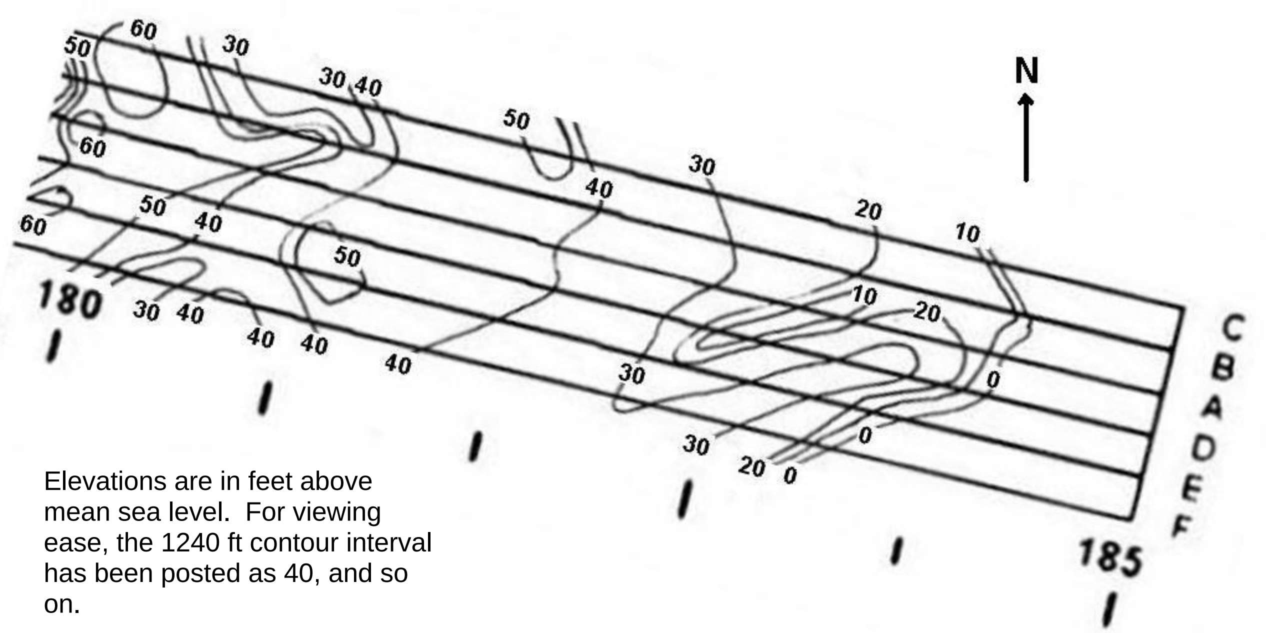

Figure 10d: Contoured top of bedrock elevation map. Segment 4 of 4 (Station 180+00 to Station 185+00; Figure 1). Elevations were posted at 25 ft intervals, hence some of the small-scale features observed on the respective resistivity profiles may not be present on the contoured map. To enhance the quality of the display, the extremely tight contour values associated with fractures that extend below the base of zone imaged on the resistivity profiles are not shown.

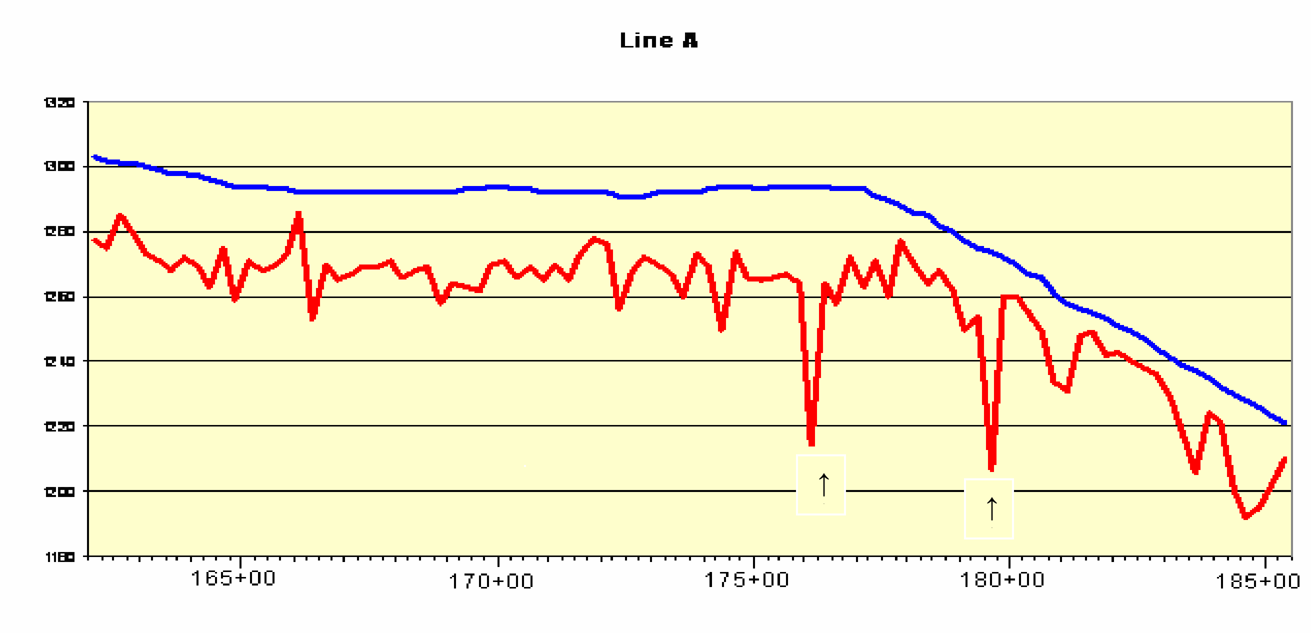

Figure 11a: Ground surface (blue) and bedrock (red) elevation (feet above mean sea level) along profile A (Figure 1). Elevations were plotted at 25 ft intervals; hence some of the small-scale features observed on the respective resistivity profile may not be present on this cross-section. The superposed arrows mark fractures that extend below the base of zone imaged on the resistivity profiles.

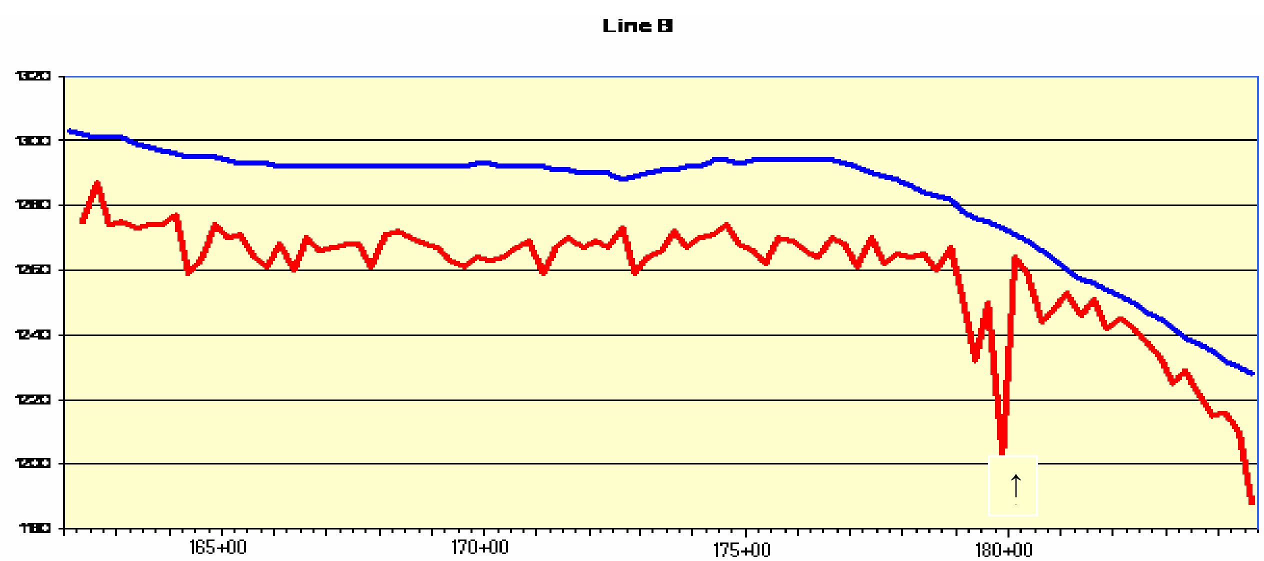

Figure 11b: Ground surface (blue) and bedrock (red) elevation (feet above mean sea level) along profile B (Figure 1). Elevations were plotted at 25 ft intervals; hence some of the small-scale features observed on the respective resistivity profile may not be present on this cross-section. The superposed arrows mark fractures that extend below the base of zone imaged on the resistivity profiles.

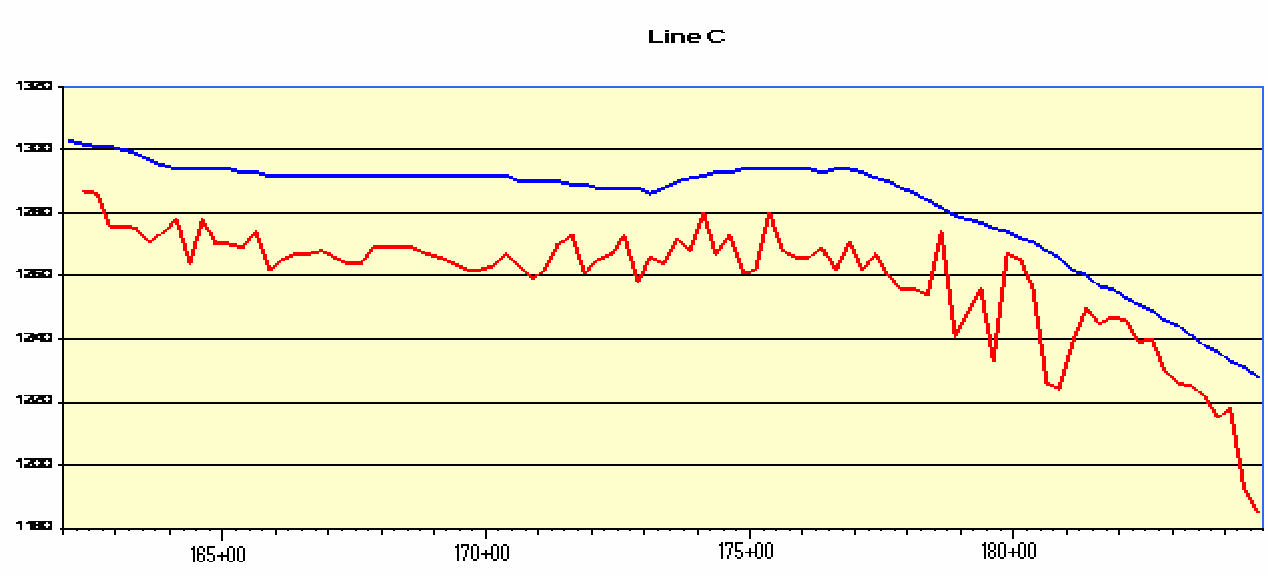

Figure 11c: Ground surface (blue) and bedrock (red) elevation (feet above mean sea level) along profile C (Figure 1). Elevations were plotted at 25 ft intervals; hence some of the small-scale features observed on the respective resistivity profile may not be present on this cross-section. The superposed arrows mark fractures that extend below the base of zone imaged on the resistivity profiles.

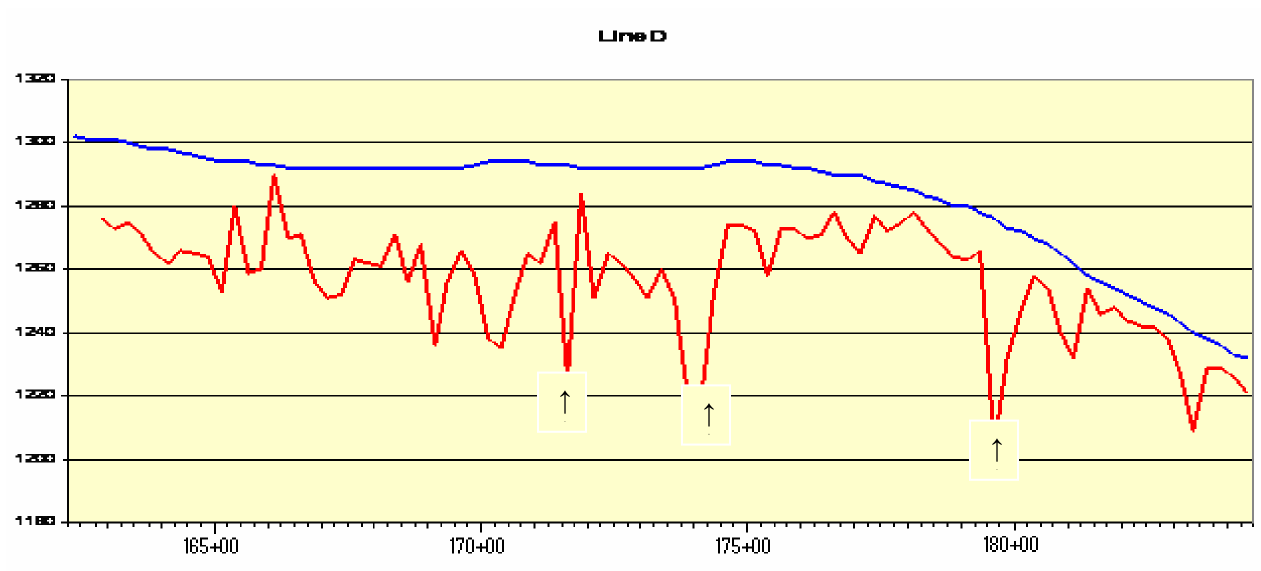

Figure 11d: Ground surface (blue) and bedrock (red) elevation (feet above mean sea level) along profile D (Figure 1). Elevations were plotted at 25 ft intervals; hence some of the small-scale features observed on the respective resistivity profile may not be present on this cross-section. The superposed arrows mark fractures that extend below the base of zone imaged on the resistivity profiles.

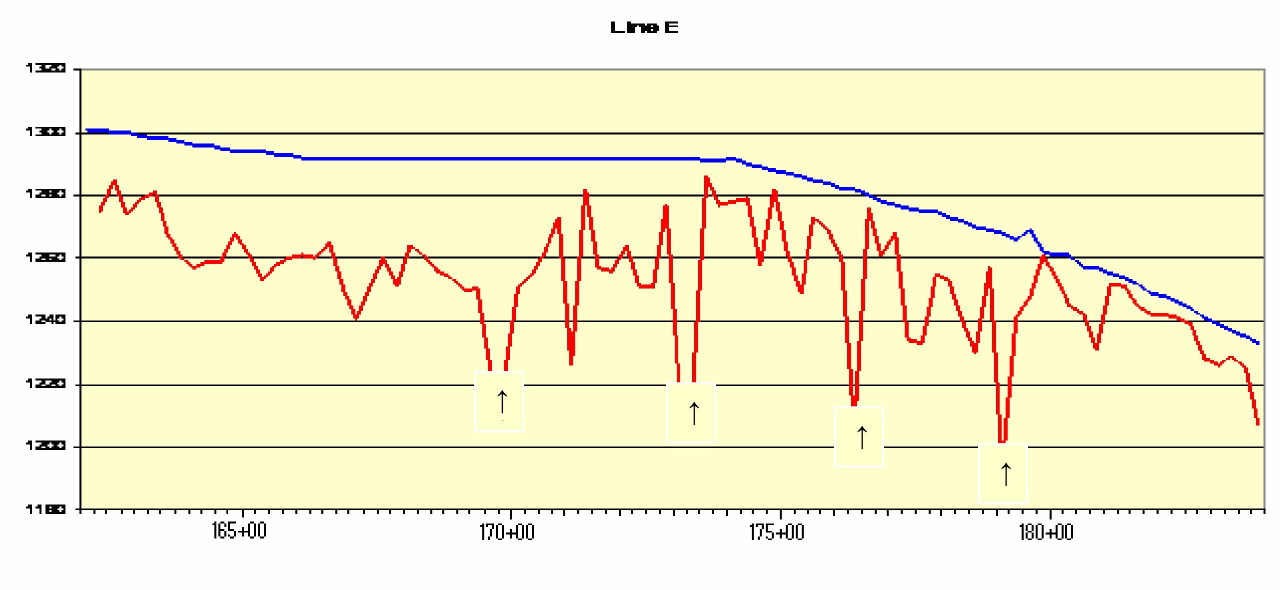

Figure 11e: Ground surface (blue) and bedrock (red) elevation (feet above mean sea level) along profile E (Figure 1). Elevations were plotted at 25 ft intervals; hence some of the small-scale features observed on the respective resistivity profile may not be present on this cross-section. The superposed arrows mark fractures that extend below the base of zone imaged on the resistivity profiles.

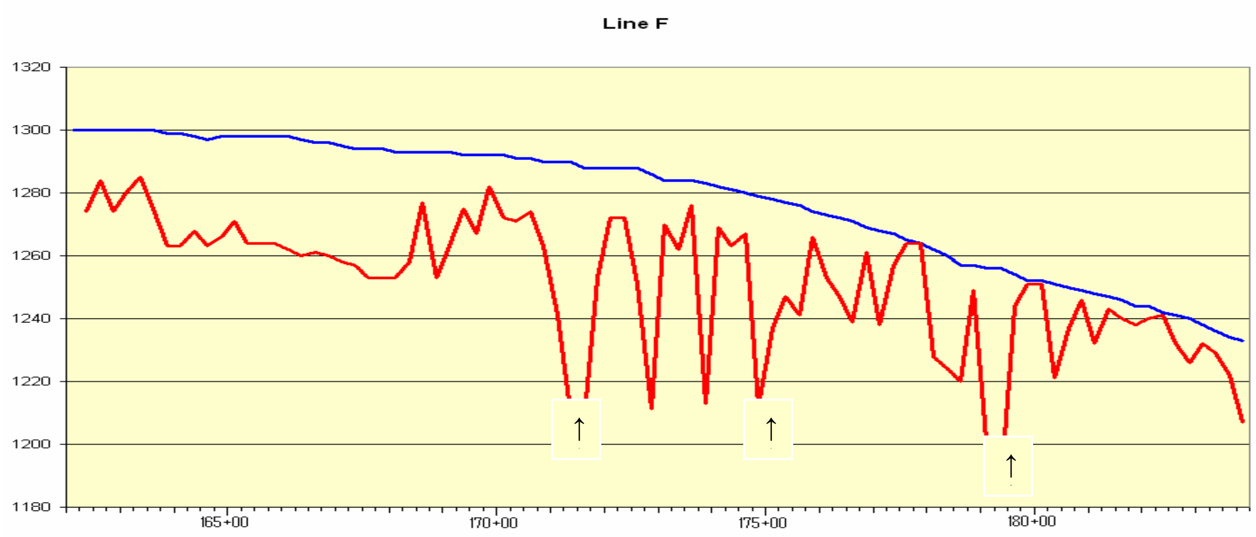

Figure 11f: Ground surface (blue) and bedrock (red) elevation (feet above mean sea level) along profile F (Figure 1). Elevations were plotted at 25 ft intervals; hence some of the small-scale features observed on the respective resistivity profile may not be present on this cross-section. The superposed arrows mark fractures that extend below the base of zone imaged on the resistivity profiles.